CERN-ACC-NOTE-2017-0034

19th May 2017
rainer.wanzenberg@desy.de

Calculation of Wakefields for the New Design of the LHCb Vertex Locator

R. Wanzenberg and O. Zagorodnova*
DESY, Notkestr. 85, 22603 Hamburg, Germany

Keywords: Wakefields, Vertex Locator, LHCb

Summary

The upgrade of the LHCb detector in the LHCb experiment was planned in 2011. The main purpose of the upgrade is an improvement of the functional abilities of the LHCb detector, such as the measurement and the collection of various characteristics of the particles produced by colliding protons. The new configuration of the LHCb detector will include an upgraded configuration of the LHCb VErtex LOcator (VELO) and a new design of the beam pipe for this detector. The wakefields for the new geometrical model of the beam pipe in the vertex locator have been calculated with the Wakefield Solver of the program CST STUDIO 2015. Preliminary results of the calculations are presented in this report.

The HiLumi LHC Design Study is included in the High Luminosity LHC project and is partly funded by the European Commission within the Framework Programme 7 Capacities Specific Programme, Grant Agreement 284404.

1 Introduction

1.1 New design of the LHCb experiment and vertex locator

A design study for the upgraded LHCb experiment was started with the goal to improve the functional abilities of the LHCb detector. In the Letter of Intent (LoI) for the LHCb Upgrade [1] the upgrade of the detector was planned to obtain output rates of up to 40 MHz [2]. The current LHCb detector has a limit of about 1fb^{-1} per year in data measurement. The upgraded detector will allow a large increase in data rate - it would collect 5fb^{-1} per year, and also will facilitate recording protons collision data at $\sqrt{s} = 14$ TeV with an instantaneous luminosity of $2 \times 10^{33}\text{cm}^{-2}\text{s}^{-1}$.

*affiliated with DESY until 2015

The physics motivations of the upgrade and proposed detector modifications are described in the Letter of Intent [1] and also in the LHCb Upgrade Framework TDR [2]. Global upgrade of the LHCb detector is scheduled during the Long Shutdown of the LHC in 2018-2019.

The new configuration of the LHCb detector will include an upgraded configuration of the LHCb sub-detector VErtex LOcator (VELO) and the silicon vertex detector that surrounds the interaction region at the LHCb. The upgraded VELO system is described in details in the LHCb VELO Upgrade TDR [3]. A 3D view of the VELO detector is shown in Fig. 1.

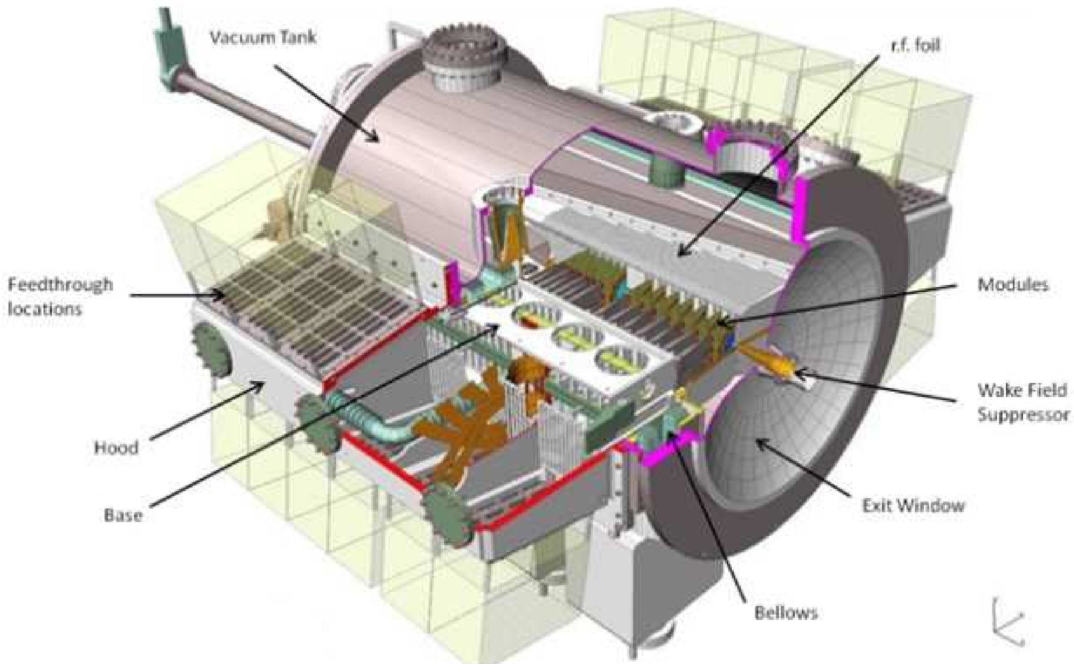

Figure 1: A 3D view of the vertex locator (VELO) in the LHCb experiment.

The new machine configuration of the VELO detector will include also changes of the geometric dimensions of the beam pipe.

1.2 Description of the geometrical model of the vertex locator in the beam pipe region

Two RF foils are installed in the VELO beam pipe region. The RF foils can be characterized as two large rectangular boxes of length $\approx$ 1 m. In the closed configuration they form the beam pipe of the LHC accelerator. A 3D view of the installed RF foils in the closed configurations is shown in Fig. 2 a) and a 3D CAD model of the RF foils is shown in Fig. 2 b).

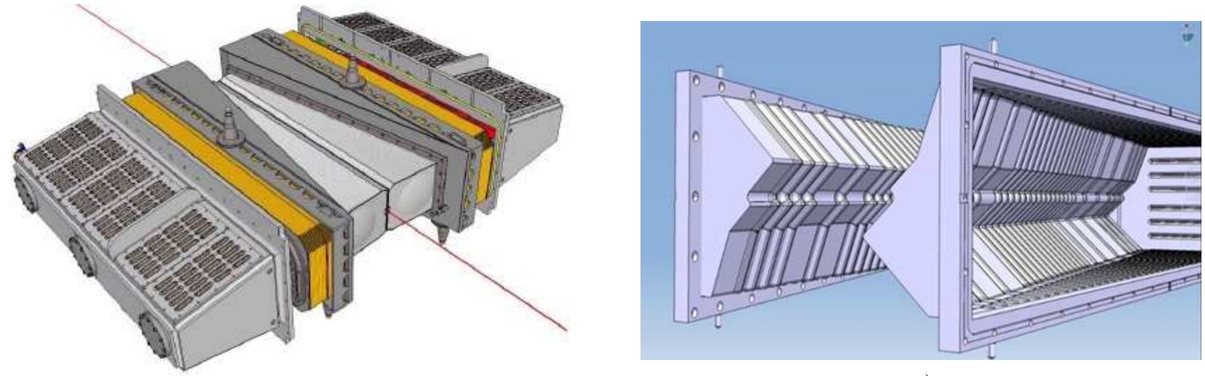

a) b)

Figure 2: A 3D view of the RF foils in the VELO detector: a) installed RF foils, b) 3D CAD model of the RF foils.

The geometrical dimensions of the RF foils will be changed for the new design of the VELO detector. The aperture of the beam pipe will be reduced from r=5.5 mm in the current design to r=3.5 mm in the new design. A view of the aperture of the VELO beam pipe is shown in Fig. 3.

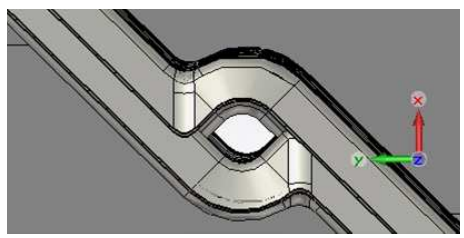

Figure 3: Aperture of the beam pipe for the new design of the VELO detector.

The wakefield suppressors connect the movable RF foils to the fixed LHC beam pipe. One of such connections is shown in Fig. 4.

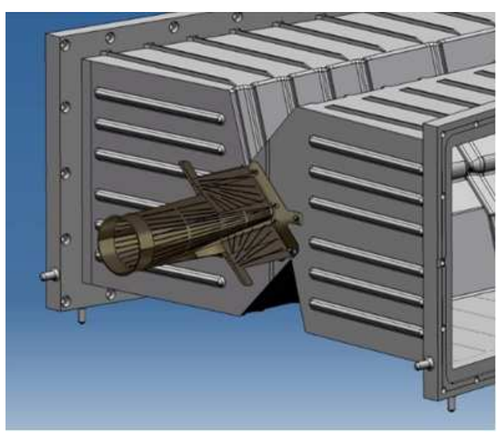

Figure 4: Connection of the RF foils to the LHC beam pipe.

2 Wakefield calculations for the VELO detector

2.1 Description of the geometrical model

A 3D CAD model of the detector from the CATIA system was used as the basis for wakefield calculations with the CST STUDIO 2015 [4]. In the model only a limited region ($x_{min} = -40$ mm, $x_{max} = 40$ mm, $y_{min} = 95$ mm, $y_{max} = 190$ mm) in the x-y-directions was used for the calculations. In the z-direction the region of the RF foils with the length of about 108 cm was used.

The imported CAD model is complemented with tapered transitions at both ends, which connect the central part with a round beam pipe with a radius of 27 mm. The tapered transitions are modeled within the CST STUDIO. These transitions are used in the model as replacement of the original wakefield suppressors. The length of the final model for the calculations is about 158 cm. The model is shown in Fig. 5.

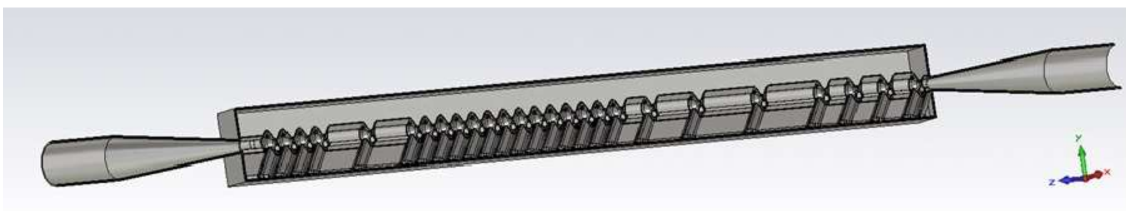

Figure 5: A 3D CST model.

2.2 Main definitions for the wakefield calculations

The wake potential [4, 5, 6] of a bunch with a charge q_1 is defined as:

$$\vec{W}(r_1, s) = \frac{1}{q_1} \int_{-\infty}^{\infty} dz \left[\vec{E}(r_1, z, t) + c\, \vec{e}_z \times \vec{B}(r_1, z, t) \right]_{t=(z+s)/c}. \tag{1}$$

The change of momentum on a test charge q_2, which is at a distance s behind the excitation bunch q_1, is given by:

$$\Delta \vec{p} = \frac{1}{c} q_1 q_2 \vec{W}(s). \tag{2}$$

The components of the wake potential $W_z(x, y, z)$, $W_x(x, y, z)$, $W_y(x, y, z)$ can be represented via Taylor expansions:

$$W_z(x, y, z) \approx W_z(0, 0, z) + \frac{\partial W_z(0, 0, z)}{\partial x} \cdot x + \frac{\partial W_z(0, 0, z)}{\partial y} \cdot y + O(2). \tag{3}$$

$$W_x(x, y, z) \approx W_x(0, 0, z) + \frac{\partial W_x(0, 0, z)}{\partial x} \cdot x + \frac{\partial W_x(0, 0, z)}{\partial y} \cdot y + O(2). \tag{4}$$

$$W_y(x, y, z) \approx W_y(0, 0, z) + \frac{\partial W_y(0, 0, z)}{\partial x} \cdot x + \frac{\partial W_y(0, 0, z)}{\partial y} \cdot y + O(2). \tag{5}$$

The longitudinal wake potential is the first term in the Taylor expansion (see Eq.(3)):

$$W_{||}^{(0)}(z) = W_z(0,0,z). \tag{6}$$

The total loss parameter can be obtained with the help of the following formula:

$$k_{||\text{tot}}^{(0)} = \int_{-\infty}^{\infty} \lambda(s) W_{||}^{(0)}(s) ds, \tag{7}$$

where $\lambda(s)$ is the normalized charge density of the bunch:

$$\lambda(s) = \frac{1}{\sigma\sqrt{2\pi}} \exp\left(-\frac{1}{2}\left(\frac{s}{\sigma}\right)^2\right). \tag{8}$$

The longitudinal monopole wake impedance is defined as Fourier transformation of the longitudinal wake potential:

$$Z_{||}(\omega) = -\frac{\int_{-\infty}^{\infty} W_{||}(s) e^{-i\omega s} ds}{\int_{-\infty}^{\infty} \lambda(s) e^{-i\omega s} ds}. \tag{9}$$

2.3 Results of the wakefield calculations with CST STUDIO

Numerical calculations in the time domain have been done with the Wakefield Solver of the program CST STUDIO 2015 [4]. The geometrical model for the calculations is a 3D model in xyz-coordinate system. It is a large structure, containing details with small geometrical dimensions. The radius of the outgoing/ingoing pipe (27 mm) and the minimal radius of the beam pipe (3.5 mm) differ by almost one order of magnitude. In order to achieve a sufficient accuracy of the calculations a fine meshing with a large number of mesh cells is required. The calculations were done with different step sizes of the mesh, which are presented in the Table 1. The accuracy of the calculations was carefully checked. The maximal number of the mesh cells is defined by the available memory of the computer.

	Δx/cm	Δy/cm	Δz/cm
1	1	1	2
2	0.5	0.5	1
3	0.2	0.5	1
4	0.5	0.2	1

Table 1: Step sizes of the mesh for the calculations with CST STUDIO [4].

Since the VELO structure is a concave structure (the aperture of the beam pipe in the central region of the structure is smaller than the aperture of the ingoing/outgoing pipe), the indirect interfaces method of wake integration [7] was used for the computations in the CST STUDIO.

The wakefield calculations have been done for the beam positions on the z-axis and with an offset 1.5 mm (x-offset or y-offset) from the z-axis to obtain all required components of the wake potential from Eqs.(3), (4) and (5).

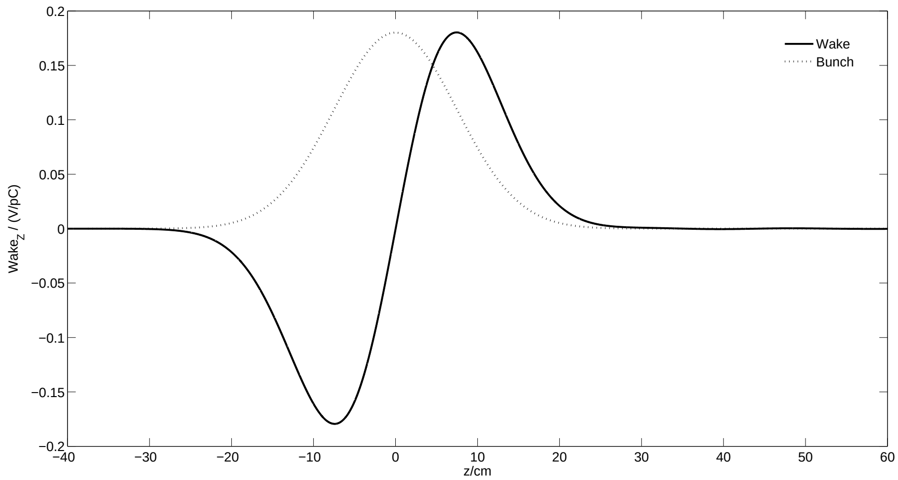

Figure 6: Longitudinal monopole wake potential $W_z(0, 0, z)$ (see Eq.(3)). The wake has been calculated for an rms bunch length of 7.5 cm. Step sizes of $\Delta x = 0.2$ mm, $\Delta y = 0.5$ mm, $\Delta z = 1$ mm were used for the calculation. The bunch shape is also shown (in arbitrary units).

The longitudinal monopole wake potential, the first term $W_z(0, 0, z)$ in the Eq.(3), is shown in Fig. 6. The wake potential was obtained for a Gaussian bunch shape with an rms bunch length of 7.5 cm. The results of the calculations of the monopole wake potential do not differ for the mesh sizes listed in Table 1 for a range of $100 \cdot \sigma_z$ behind the bunch. The loss parameter $k^{(0)}_{||\text{tot}}$ is about $2.5 \cdot 10^{-5}$ V/pC.

The transverse x-component of the wake potential, the first term $W_x(0, 0, z)$ in the Eq.(4), is shown in Fig. 7. The transverse y-component, the first term $W_y(0, 0, z)$ in the Eq.(5), is shown in Fig. 8. These components were obtained as results of wakefield calculations with beam position on the z-axis for a Gaussian bunch shape with an rms bunch length of 7.5 cm for different mesh sets with minimal possible mesh sizes. Step sizes $\Delta x = 0.5$ mm, $\Delta y = 0.5$ mm, $\Delta z = 1$ mm have been used for the calculation of the Wake1 and step sizes $\Delta x = 0.2$ mm, $\Delta y = 0.5$ mm, $\Delta z = 1$ mm for the calculation of the Wake2 in Fig. 7. Step sizes $\Delta x = 0.5$ mm, $\Delta y = 0.5$ mm, $\Delta z = 1$ mm have been used for the calculation of the Wake1 and step sizes $\Delta x = 0.5$ mm, $\Delta y = 0.2$ mm, $\Delta z = 1$ mm for the calculation of the Wake2 in Fig. 8.

The accuracy of the calculations of the transverse components of the wake potential, especially the x-component, is not sufficient.

The partial derivatives in the Eqs. (3), (4) and (5) can be obtained approximately with the help of the formulas:

$$\frac{\partial W(0, 0, z)}{\partial x} \approx \frac{W(h_x, 0, z) - W(0, 0, z)}{h_x}, \tag{10}$$

$$\frac{\partial W(0, 0, z)}{\partial y} \approx \frac{W(0, h_y, z) - W(0, 0, z)}{h_y}. \tag{11}$$

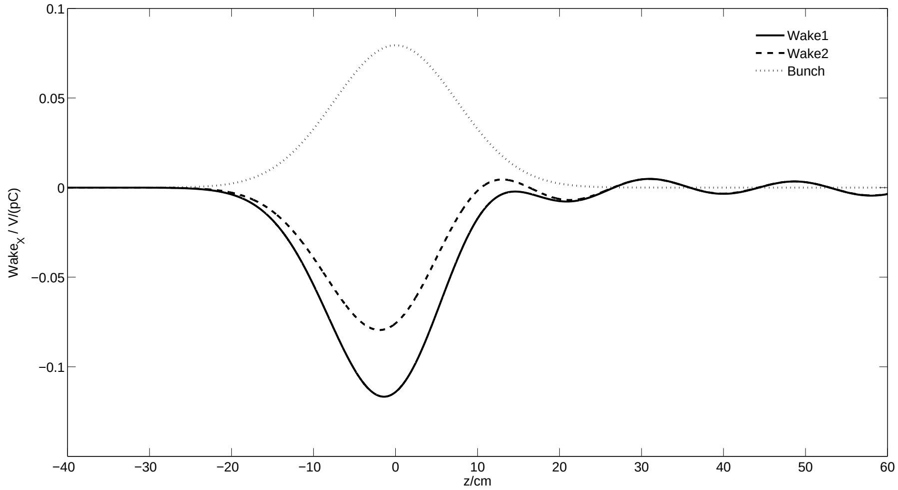

Figure 7: Transverse component (x-component) of the wake potential $W_x(0,0,z)$ (see Eq.(4)) for different mesh sizes for an rms bunch length of 7.5 cm. The bunch shape is also shown (in arbitrary units).

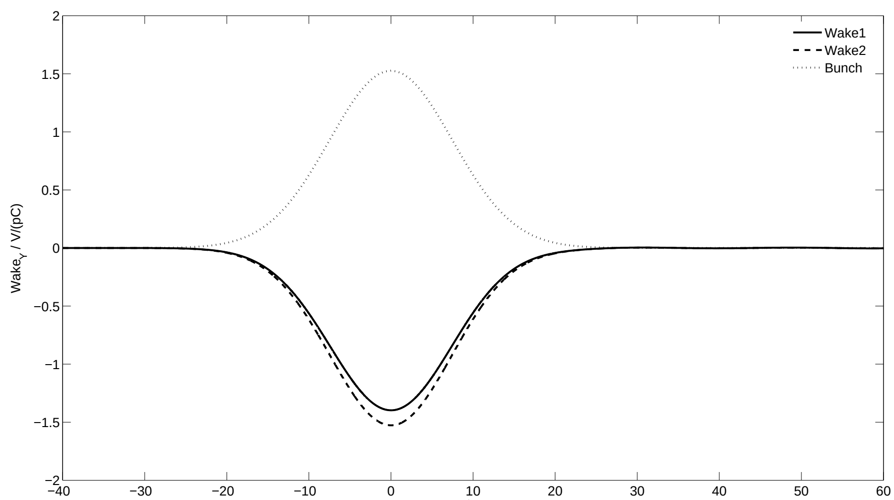

Figure 8: Transverse component (y-component) of the wake potential $W_y(0,0,z)$ (see Eq.(5)) for different mesh sizes for an rms bunch length of 7.5 cm. The bunch shape is also shown (in arbitrary units).

In order to obtain the second and the third terms in the Eqs. (3), (4) and (5) the wakefield calculations for the beam position with an offset from the z-axis have been done for two cases: x-offset $h_x = 1.5$ mm and y-offset $h_y = 1.5$ mm.

The accuracy of the calculations also depend on the mesh properties in case of off-axis calculations. The results of these calculations are represented for the meshes with minimal possible step sizes.

The components $\partial W_z(0,0,z)/\partial x$, $\partial W_z(0,0,z)/\partial y$ from equation (3) are shown in Fig. 9 and Fig. 10. The components $\partial W_x(0,0,z)/\partial x$, $\partial W_x(0,0,z)/\partial y$ from equation (4) are shown in Fig. 11 and Fig. 12, and the components $\partial W_y(0,0,z)/\partial x$, $\partial W_y(0,0,z)/\partial y$ from equation (5) in Fig. 13 and Fig. 14.

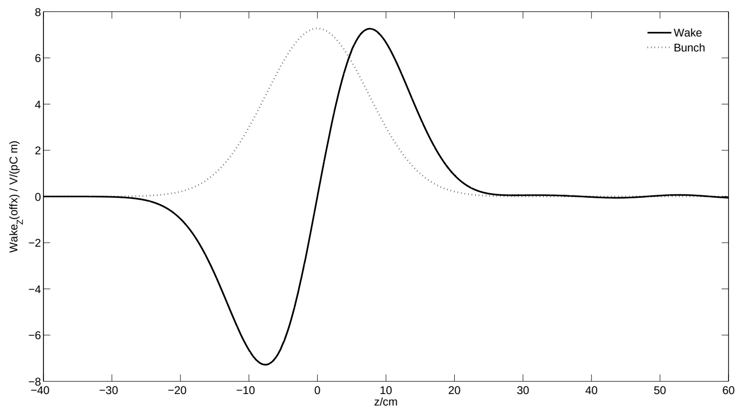

Figure 9: Component $\partial W_z(0,0,z)/\partial x$ of the wake potential from equation (3). The wake has been calculated for an rms bunch length of 7.5 cm with offset $h_x = 1.5$ mm from the x-axis. Step sizes $\Delta x = 0.2$ mm, $\Delta y = 0.5$ mm, $\Delta z = 1$ mm have been used for the calculation. The bunch shape is also shown (in arbitrary units).

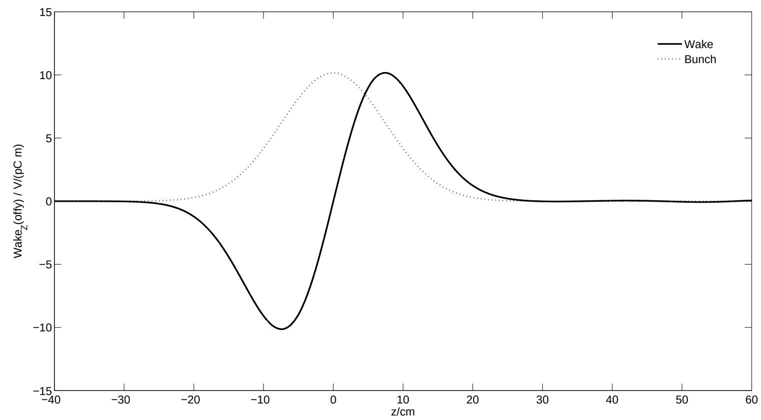

Figure 10: Component $\partial W_z(0,0,z)/\partial y$ of the wake potential from equation (3). The wake has been calculated for an rms bunch length of 7.5 cm with offset $h_y = 1.5$ mm from the y-axis. Step sizes $\Delta x = 0.5$ mm, $\Delta y = 0.2$ mm, $\Delta z = 1$ mm have been used for the calculation. The bunch shape is also shown (in arbitrary units).

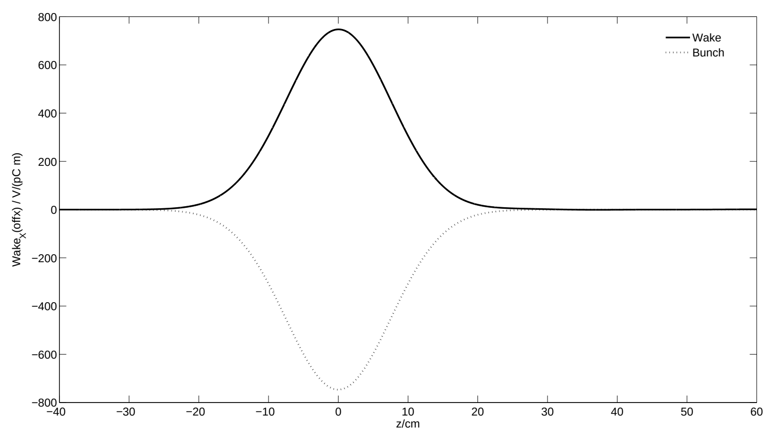

Figure 11: Component $\partial W_x(0,0,z)/\partial x$ of the wake potential from equation (4). The wake has been calculated for an rms bunch length of 7.5 cm with offset $h_x = 1.5$ mm from the x-axis. Step sizes $\Delta x = 0.2$ mm, $\Delta y = 0.5$ mm, $\Delta z = 1$ mm have been used for the calculation. The bunch shape is also shown (in arbitrary units).

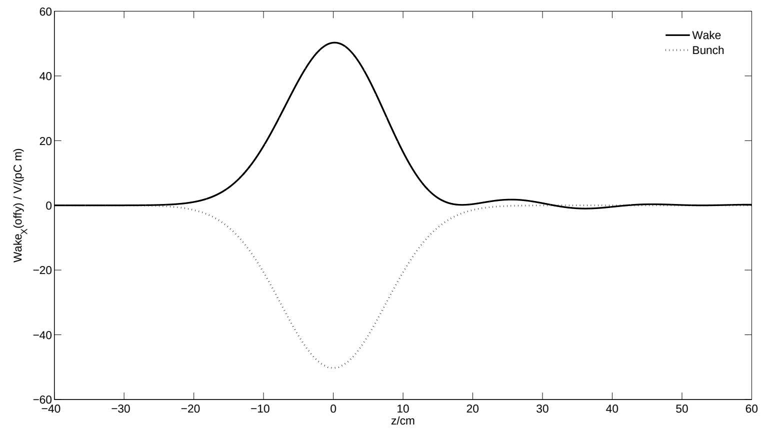

Figure 12: Component $\partial W_x(0,0,z)/\partial y$ of the wake potential from equation (4). The wake has been calculated for an rms bunch length of 7.5 cm with offset $h_y = 1.5$ mm from the y-axis. Step sizes $\Delta x = 0.5$ mm, $\Delta y = 0.2$ mm, $\Delta z = 1$ mm have been used for the calculation. The bunch shape is also shown (in arbitrary units).

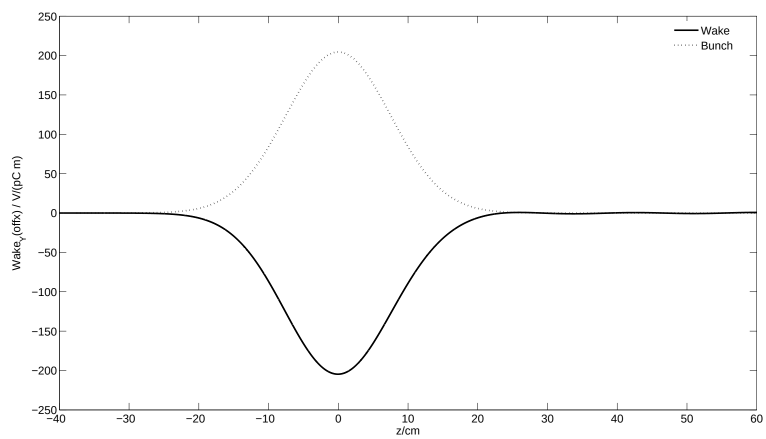

Figure 13: Component $\partial W_y(0,0,z)/\partial x$ of the wake potential from equation (5). The wake has been calculated for an rms bunch length of 7.5 cm with offset $h_x = 1.5$ mm from the x-axis. Step sizes $\Delta x = 0.2$ mm, $\Delta y = 0.5$ mm, $\Delta z = 1$ mm have been used for the calculation. The bunch shape is also shown (in arbitrary units).

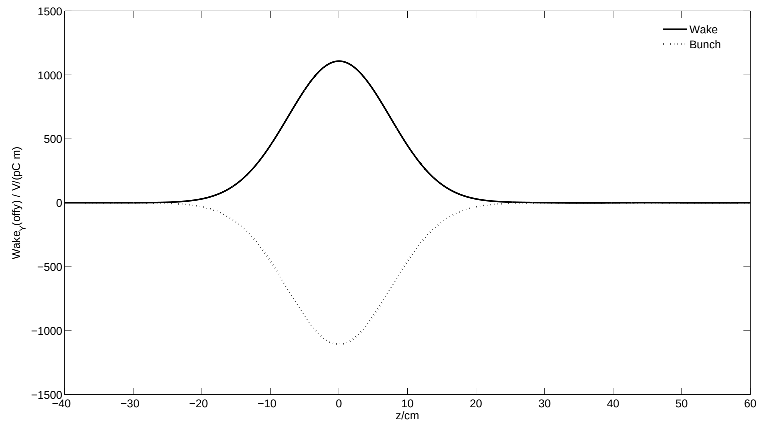

Figure 14: Component $\partial W_y(0,0,z)/\partial y$ of the wake potential from equation (5). The wake has been calculated for an rms bunch length of 7.5 cm with offset $h_y = 1.5$ mm from the y-axis. Step sizes $\Delta x = 0.5$ mm, $\Delta y = 0.2$ mm, $\Delta z = 1$ mm have been used for the calculation. The bunch shape is also shown (in arbitrary units).

2.4 Results of the impedance calculations with the CST STUDIO

The wakefield calculations with a beam position on the z-axis for a Gaussian bunch with an rms bunch length of 1 cm have been done to obtain the longitudinal wake potential for a range of $1000 \cdot \sigma_z = 10$ m behind the bunch and the longitudinal impedance for this wake potential. The accuracy of the calculations was checked for different step sizes of the mesh from the Table 1. The results of the calculation of the wake potential do not differ for the wakes with a length of less than $100 \cdot \sigma_z$. The longitudinal monopole wake potential for a Gaussian bunch with an rms bunch length of 1 cm is shown in Fig. 15 for two different step sizes of the mesh in the range until 2.5 m. Real and imaginary parts of the longitudinal impedance were obtained as results of the post-processing in the CST STUDIO. They are shown in Fig. 16 and Fig. 17.

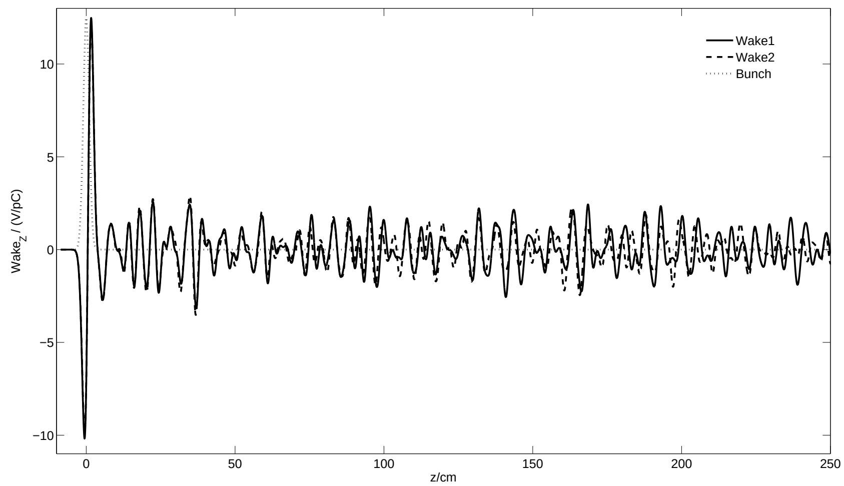

Figure 15: Comparison of the longitudinal monopole wake potential for the VELO structure which has been calculated with different mesh sizes for a bunch with an rms bunch length of 1 cm. For the calculation of the Wake1 step sizes of $\Delta x = 0.5$ mm, $\Delta y = 0.5$ mm, $\Delta z = 1$ mm have been used. For the calculation of the Wake2 step sizes of $\Delta x = 0.2$ mm, $\Delta y = 0.5$ mm, $\Delta z = 1$ mm have been used. The bunch shape is also shown (in arbitrary units).

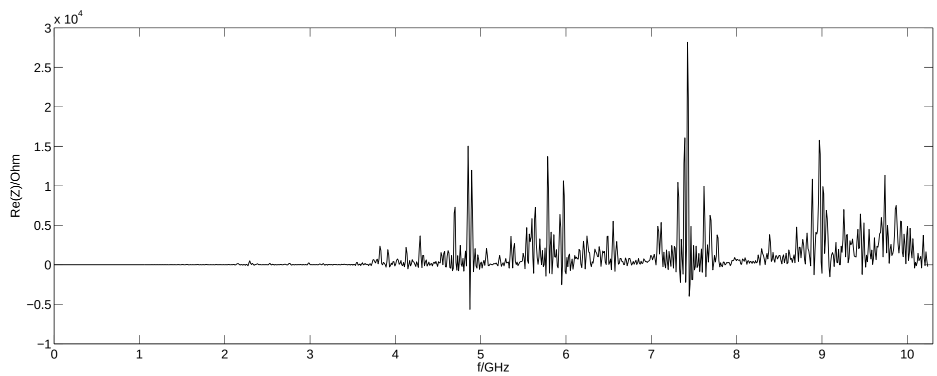

Figure 16: Real part of the longitudinal impedance for the VELO structure. The impedance was calculated with the CST STUDIO for a Gaussian bunch with an rms bunch length of 1 cm. Step sizes $\Delta x = 0.2$ mm, $\Delta y = 0.5$ mm, $\Delta z = 1$ mm have been used for the calculation.

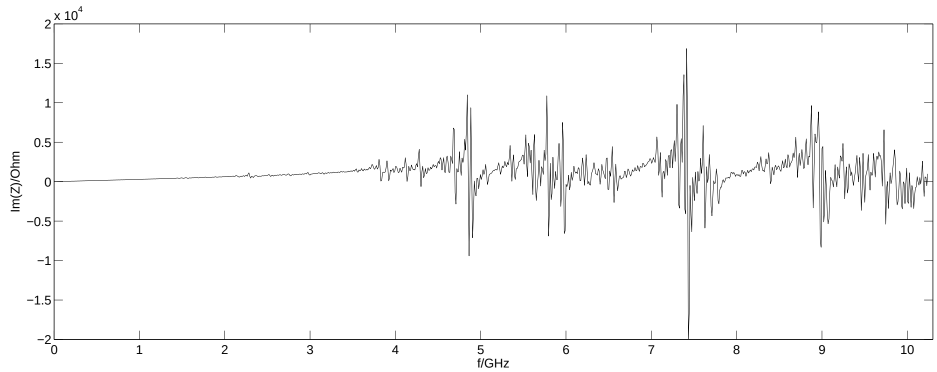

Figure 17: Imaginary part of the longitudinal impedance for the VELO structure. The impedance was calculated with the CST STUDIO for a Gaussian bunch with an rms bunch length of 1 cm. Step sizes $\Delta x = 0.2$ mm, $\Delta y = 0.5$ mm, $\Delta z = 1$ mm have been used for the calculation.

3 Wakefield calculations for the rotationally symmetric model

Two rotationally symmetric models, a three-dimensional and a two-dimensional, were developed to estimate the accuracy of the wakefield calculations for the VELO structure. The three-dimensional model is shown in Fig. 18, and the two-dimensional model - in Fig. 19.

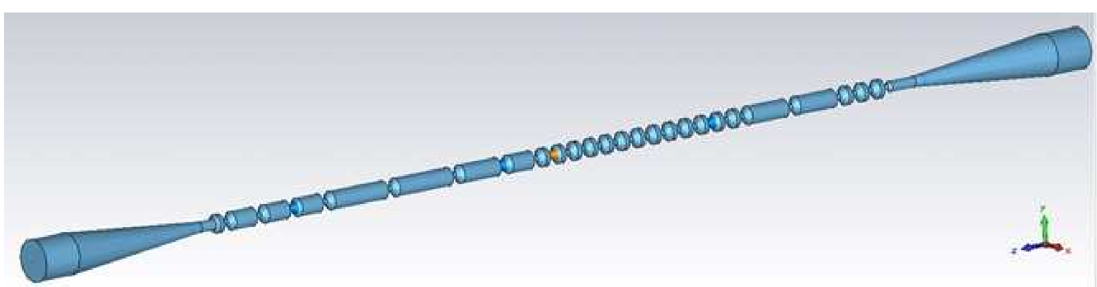

Figure 18: Three-dimensional approximate model.

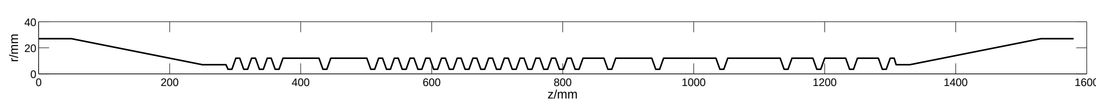

Figure 19: Two-dimensional approximate model. All dimensions are given in mm.

The geometrical dimensions of the rotationally symmetric models are approximated to the dimensions of the VELO structure. The minimal radius of the beam pipe is equal to 3.5 mm and the radius of the ingoing and outgoing pipes is 27 mm. Wakefield calculations for the 3D-model have been done with the program CST STUDIO [4], while for the 2D-model the program ECHO2D [7, 8] has been used for a Gaussian bunch with an rms bunch length of $\sigma_z = 7.5$ cm. Different mesh properties were used to estimate the accuracy of the calculations. It is possible to use very fine meshes in the computations for the two-dimensional model. Longitudinal monopole wake potentials and transverse dipole wake potentials were obtained as results of the 3D-calculations and the 2D-calculations. The results for the longitudinal and for the transverse wake potentials of 2D calculations with the ECHO2D code are independent of the mesh properties. The accuracy of the calculations of the longitudinal wake potential in the CST STUDIO is also very good for different mesh properties. The accuracy of the calculations of the transverse wake potential seems to be sufficient, but the difference between 2D and 3D results for the transverse wake potential is significant.

A comparison of the longitudinal wake potentials, resulting from the 3D calculations and from 2D calculations, is shown in Fig. 20, and a comparison of the transverse wake potentials is shown in Fig. 21. The transverse wake potential in Fig. 21 is shown also for two different meshes for the 3D calculations.

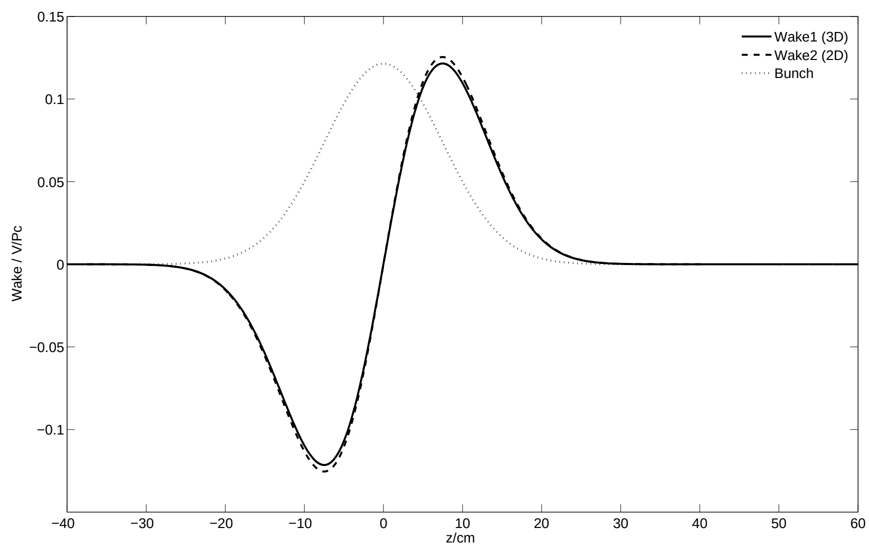

Figure 20: Longitudinal monopole wake potential for the rotationally symmetric approximate structure. The Wake1 was obtained for the three-dimensional model (step sizes: $\Delta x = 0.5$ mm, $\Delta y = 0.5$ mm, $\Delta z = 1$ mm). The Wake2 was obtained for the two-dimensional model (step sizes: $\Delta r = 0.5$ mm, $\Delta z = 1$ mm). The bunch shape is also shown (in arbitrary units).

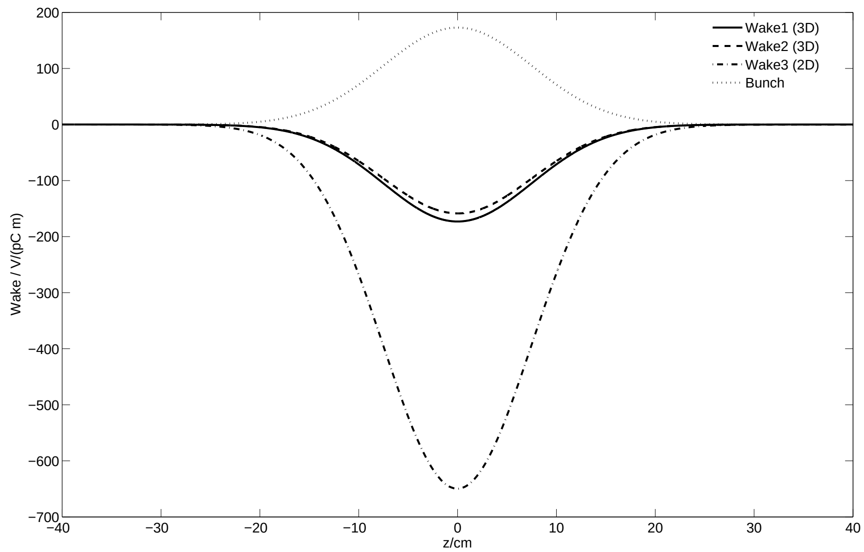

Figure 21: Transverse dipole wake potential for the rotationally symmetric approximate structure. The Wake1 and Wake2 were obtained for the three-dimensional model (step sizes for the Wake1: $\Delta x = 0.5$ mm, $\Delta y = 0.5$ mm, $\Delta z = 1$ mm; for the Wake2: $\Delta x = 0.2$ mm, $\Delta y = 0.2$ mm, $\Delta z = 0.5$ mm). The Wake3 was obtained for the two-dimensional model (step sizes: $\Delta r = 0.2$ mm, $\Delta z = 0.5$ mm). The bunch shape is also shown (in arbitrary units).

4 Summary

The short range wakefields for the new design of the LHCb VELO have been calculated with help of the Wakefield Solver of the program CST STUDIO 2015 [4]. A three-dimensional model of the VELO, imported in the CST STUDIO from the CATIA system and processed in the CST program, was used for the calculations.

The accuracy of the calculations was estimated for longitudinal and transverse components of the wake potential. The calculations have been done for different mesh properties for beam position on the z-axis and also with offsets from the z-axis. The accuracy of the calculations is only sufficient for the longitudinal wake potential within a range of $100 \cdot \sigma_z$ behind the bunch and with the beam position on axis.

The loss parameter, obtained from the longitudinal wake potential, is very small (in the 10^{-5} to 10^{-4} V/pC range).

The real and imaginary part of the longitudinal impedance were obtained with help of the post-processor in the Wakefield Solver of the program CST STUDIO. The impedance was calculated for a Gaussian bunch with an rms bunch length of 1 cm.

To get a better understanding of the accuracy problem of the wakefield calculations for the VELO detector a simplified rotationally symmetric model was used for 2D calculations and for 3D calculations. 2D calculations have been done with the ECHO2D code [7, 8]. The 3D model was developed in the CST STUDIO and calculations for this model have been done with the CST STUDIO. The accuracy of the results is sufficient for the longitudinal wake potential and not sufficient for the transverse wake potential.

Therefore, the 3D based model of the VELO detector and the simplified rotationally symmetric model are very complicated for the calculations since they contain details with small geometrical dimensions. The minimal aperture of the beam pipe is very small. The convergence of the results of the wakefields calculations is slow.

The results for the 3D calculations of the transverse wake potential differ from the results for the 2D calculations by a factor of four (see. Fig. 21). Further investigations are needed to clarify this issue.

Acknowledgment

We would like to thank Massimiliano Ferro-Luzzi, Elias Métral and Benoit Salvant for useful discussions and comments on this work.

References

[1] LHCb collaboration, *Letter of Intent for the LHCb Upgrade*, CERN-LHCC-2011-001, LHCC-I-018

[2] LHCb collaboration, *Framework TDR for the LHCb Upgrade: Technical Design Report*, CERN-LHCC-2012-007. April, 2012

[3] LHCb collaboration, *LHCb VELO Upgrade Technical Design Report*, CERN-LHCC-2013-021. November, 2013

[4] *CST STUDIO 2015* is trademark of CST AG, Buedinger Str. 2a, 64289 Darmstadt, Germany.

[5] T. Weiland, R. Wanzenberg, *Wakefields and Impedances*, in: Joint US-CERN part. acc. school, Hilton Head Island, SC, USA, 7 - 14 Nov 1990 / Ed. by M Dienes, M Month and S Turner. - Springer, Berlin, 1992- (Lecture notes in physics ; 400) - pp.39-79.

[6] T. Weiland, *On the numerical solution of Maxwell's Equations and Applications in the Field of Accelerator Physics*, Part. Acc. 15 (1984), 245-292.

[7] I. Zagorodnov, *Indirect methods for wake potential integration*, Phys. Rev. ST Accel. Beams **9** (2006) 102002 [arXiv:physics/0606049].

[8] I. Zagorodnov and T. Weiland, *TE/TM field solver for particle beam simulations without numerical Cherenkov radiation*, Phys. Rev. ST Accel. Beams **8** (2005) 042001.